Chapter 3 : Procedures and Techniques

3.1 VT DGV Procedures and Techniques

This chapter will discuss the procedures and techniques used to align the optics in each of the camera modules, calibrate and run the calibration wheel, acquire the various correction images needed to reduce raw DGV data images into DGV velocity data, acquire calibration images needed to determine the absorption characteristics of each iodine cell used in the VT DGV system, and acquire the raw DGV data images. The only significant change made during this research to the procedures used to acquire the correction, calibration, and data images was to add a procedure to acquire a series of images used in calculating Euler angles for each camera module that were then in turn used to calculate the unit vector $\hat{a}$ in equation 1. Proper alignment of the optics in the camera modules allowed the maximum image area to be used as the Regions of Interest (ROI's) while acquiring and reducing DGV data. The calibration wheel was used in this research as a way of independently verifying the performance of the VT DGV system. The VT DGV system acquired velocity data while viewing the calibration wheel as the wheel rotated at a known angular velocity. The reduced VT DGV data could then be compared to the known rectilinear velocity profile of the calibration wheel. Several different types of correction images are needed to account for various types of image imperfections inherent to the acquired data images. These imperfections occur for a variety of reasons. Two examples of image imperfections are non uniform sensitivity of the light collecting pixels in the Charge Coupled Device (CCD) inside each camera and stray ambient light collected by the cameras during data acquisition. Calibration images are needed to determine the absorption properties of the iodine cells used in the DGV system. These images can then be compared to the

theoretical absorption properties of an iodine cell of the same size and vapor pressure to determine how the absorption properties of the iodine cells vary with the optical frequency of the light passing through the cell. Once all of the correction images and calibration images have been acquired, the raw DGV data images can be acquired.

3.2 Camera Module Optics Alignment

An apparatus has been developed to align the optics inside each camera module. Proper alignment of the optics inside each module insures that the maximum viewing area is available for data collection. Figure 3.1 shows one of the camera modules during optics alignment. A Coherent© Diode Laser was used to perform the rough alignment of the optics. The diode laser was placed roughly 42 inches away from the front of the camera module. A mechanism was designed to hold and position the laser head so the beam hit the center of the first image acquisition mirror. The diode laser head was aligned so that the beam, emitted from this laser, reflected off of a mirror attached to the front edge of the camera module and back to the center of the front face of the laser head. This ensured that the beam was perpendicular to the front edge of the camera module. Next, the laser alignment mirror was removed from the front of the camera module and the laser was fired into the module toward a target placed on the lens cap of the camera. The laser beam was split by the optics inside the module and module optics were adjusted until the two beams projected on the lens cap target were equally spaced roughly 3/16 inch from a center line placed on the lens cap target. Next, the laser was turned off, the lens cap and lens cap target were removed from the camera and images were acquired of the diode laser head. The positions of the optics were adjusted until the distances from the split line between the two images to the center of the laser head on each image were equal. Finally, the positions of the optics were fine-tuned until the center of the laser head was centered horizontally in each of the fields of view.

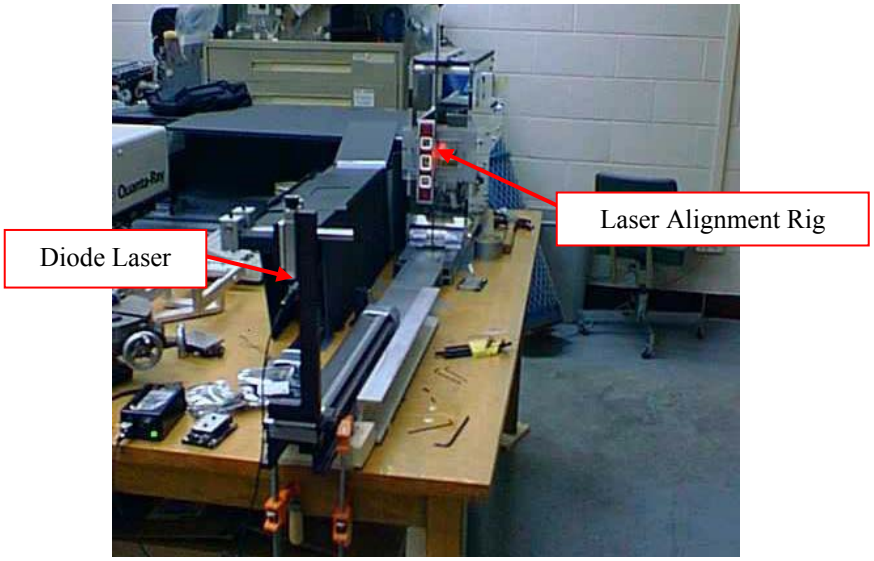

Figure 3.1: Camera module optics alignment apparatus

3.3 Calibrating the Calibration Wheel

The calibration wheel was run through a series of tests to determine the relationship between the voltage output by the Baldor Smartmove controller to the wheel speed in revolutions per second. The data needed to determine this relationship were acquired by running the wheel for 10 seconds at 5 rev/s increments from -65 rev/s to 65 rev/s as well as -66.7 rev/s and 66.7 rev/s and capturing an array of velocity data and an array of voltage data for each speed. The array of velocity data was acquired by the controller itself and then downloaded to the host computer. The voltage data were acquired by the data acquisition card in DGV1. Next the average voltage and the average motor velocity were calculated and plotted. Figure 3.2 shows a plot of the average controller output voltage versus the average wheel speed. A linear regression of these data was performed to determine an equation relating the offset voltage to the wheel speed. The plot also shows this equation relating the output voltage to the wheel speed. The equation is also given below:

$$Speed = -51.2070(Voltage) - 0.2589 \qquad (3)$$

where *Speed* is the wheel speed in rev/s and *Voltage* is the offset voltage from the controller.

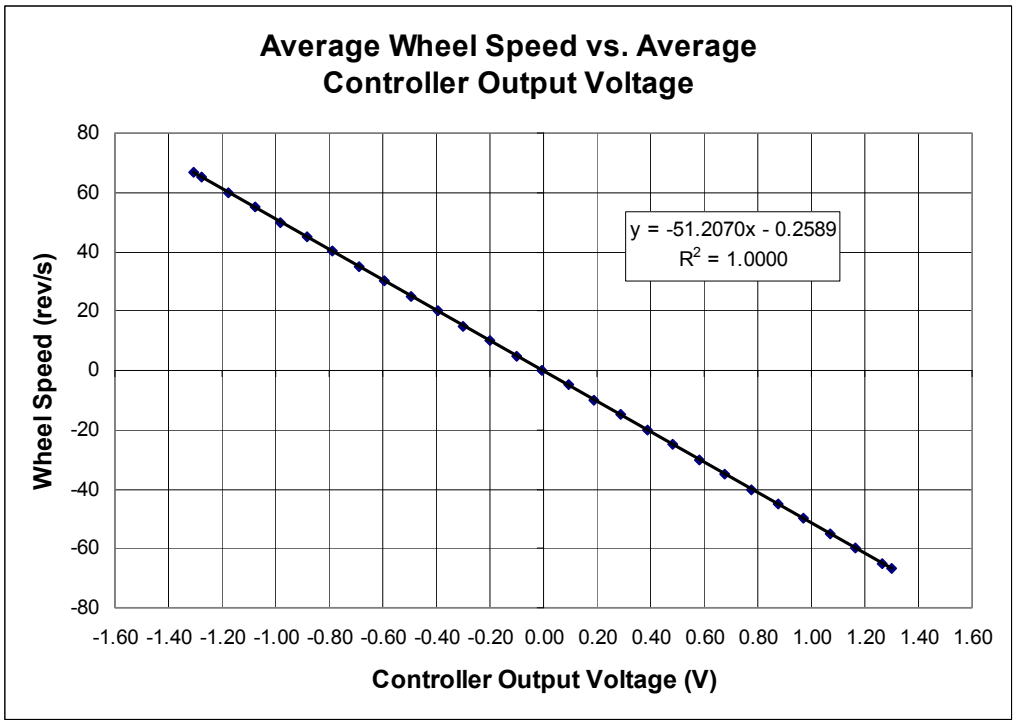

Figure 3.2: Wheel calibration plot.

3.4 Correction Images

3.4.1 Geometric Correction

Images of a dot grid or checkerboard placed in the data plane are needed when using the DGV technique. These images are used to correct for the geometric distortions that occur due to each of the camera modules viewing the data plane from a different location. During previous tests of the Virginia Tech DGV system, images of a dot grid were acquired to correct for geometric distortion. The pattern used to acquire these images was changed to a checkerboard during this research because the images of a checkerboard pattern could be directly plugged into the *"Camera Calibration Toolbox for MATLAB"*[80]. This toolbox was used to determine the viewing angles for each of the three camera modules. The checkerboard pattern was 9" x 7" in size and consisted of black and white 12.7 mm (½ inch) squares.

Prior to each iodine cell calibration or acquisition of a set of DGV velocity data, several images (between 5 and 10) of the checkerboard were acquired and averaged. The average image was used to determine the size and location of the Region of Interest (ROI) where DGV data would be collected. A warp point was selected at each of the four corners of the ROI. This region of interest appeared as a parallelogram or a trapezoid. In addition to choosing the warp points, a rectangular

region of interest proportional to the known size of the region of interest was also chosen in the Graphic User Interface of the DGV Control Program. Next the warped region of interest was mapped to the rectangular region of interest selected by the program user. This mapping is referred to as de-warping since this step removes the geometric effects of perspective from the region of interest. The reference and filtered regions of interest for each camera module were mapped separately. The region of interest for the reference view was designated Region 1 and the region of interest for the filtered view was designated Region 2. The filtered view was vertically mirrored before the warp points were selected and before the view was mapped to the corresponding rectangular region of interest. Each mapping produced an image in which the point of view appears to be perpendicular to the data plane. This type of image correction allows images acquired from multiple points of view to be overlaid on top of one another thus producing velocity data in any desired inertial reference frame. Figure 3.3 shows before and after images demonstrating the effects of mapping an image of the checkerboard to the rectangular region of interest. The selected warp points and rectangular region of interest could be saved, as part of a configuration file, for future use. More information on the techniques used to perform this mapping can be found in reference 81.

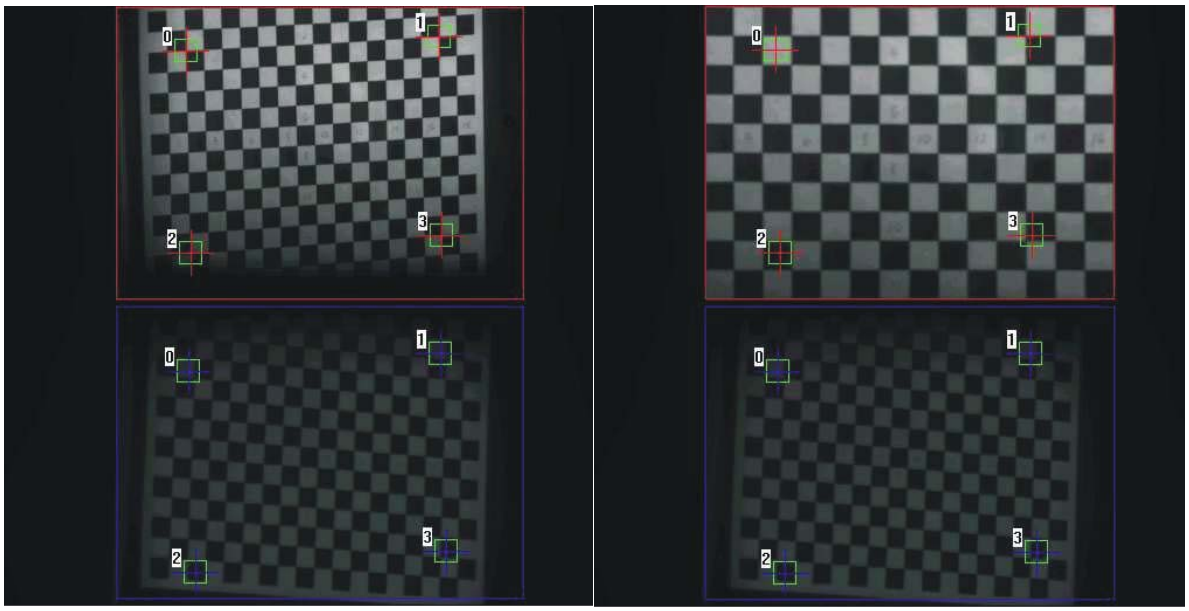

(a) (b)

Figure 3.3: Demonstration of geometric image correction. Figure (a) shows checkerboard and warp points before mapping and figure (b) shows checkerboard after mapping.

3.4.2 Background Correction

The basic premise upon which every camera functions is that the camera collects and stores light while the shutter on the camera is open. Definable images appear through variations in light

intensity reflected off of objects in the field of view of the camera. The cameras used in the Virginia Tech DGV system also function in this way, but this principal also becomes a source of signal error because the data plane is illuminated by laser light for only a very small portion of the time the camera shutter is open. Ambient light in the area where the DGV system is being used is also collected while the camera shutters are open. Since the signal used to discern velocity in the DGV technique is the light intensity collected by each pixel in the Charge Couple Device (CCD) inside the digital cameras used by the system, this ambient light causes an error in the velocities measured by the system. The solution to this problem is straight forward. Images are collected over the same period of time and under the same lighting conditions in which velocity data will be collected but the data plane is not illuminated by the laser. These "background images" are then subtracted from the data images to account for the ambient light illuminating the area where data is being taken.

Several background images (between 5 and 20) were acquired before each iodine cell calibration was performed and before each set of velocity data was acquired. The acquired background images were averaged to calculate an average background image. This average background image was subtracted from each iodine cell calibration image and each velocity data image during data reduction. All of the background images and DGV velocity data images were acquired with all of the lights in the area turned off. The ideal background condition to acquire DGV data is complete darkness. This minimizes the effect of the background image thus providing the maximum light intensity range over which data can be collected. During DGV data acquisition in the Virginia Tech Stability Wind Tunnel, the average light intensities measured by each camera during background image acquisition were roughly: 1180 for camera module 1, 1270 for camera module 2, and 990 for camera module 3. These light intensities were out of a maximum value of 65536.

3.4.3 Pixel Sensitivity Correction

Ideally the sensitivity to light of each pixel in the Charge Couple Device (CCD) array of a camera used in a DGV system should be uniform. Unfortunately this is never the case. These variations in pixel sensitivity are a potential source of measurement error in the DGV technique so a correction is needed to account for them. The procedure used to make this correction required two different sets of images of a uniformly illuminated surface to be acquired with the lens removed from the camera. The first set of images was acquired at an illumination intensity roughly 25% of the maximum light intensity discernable by the camera. The second set of images was acquired at an illumination intensity roughly 75% of the maximum light intensity discernable by the camera. Next, a pixel sensitivity factor was calculated for each pixel in the CCD array using the following formula:

$$PS_{ij} = \frac{P_{ij}^1 - P_{ij}^2}{L_1 - L_2} \tag{4}$$

where PS_{ij} was the pixel sensitivity factor for the CCD pixel at row *i* and column *j*, P_{ij}^1 was the light intensity recorded by the CCD pixel at row *i* and column *j* for the higher illumination intensity (75%), P_{ij}^2 was the light intensity recorded by the CCD pixel at row *i* and column *j* for the lower illumination intensity (25%), L_1 was the average light intensity of all CCD pixels for the higher illumination intensity (75%), and L_2 was the average light intensity of all CCD pixels for the lower illumination intensity (25%). The pixel sensitivity correction is applied to an image by dividing the image by the pixel sensitivity correction image. This operation is performed by dividing the integer light intensity value for each pixel in the image being corrected by the corresponding integer light intensity value of the corresponding pixel in the pixel sensitivity correction image.[82]

The uniformly illuminated surface was created using an extension cord with an inline dimmer switch, a desk lamp, six sheets of 6.35 mm (¼ inch) thick opaque white Plexiglas, and 6 sheets of 20 bond white copy machine paper. The 6 sheets of white paper were placed between the third and fourth sheets of Plexiglas. The desk lamp was plugged into the extension cord and the Plexiglas sheets were placed against the open end of the metal shroud covering the light bulb in the lamp. The camera was placed against the other side of the Plexiglas sheets. The dimmer switch was used to adjust the intensity of the light bulb used to illuminate the Plexiglas sheets. Figure 3.4 is a drawing showing the setup used to determine the pixel sensitivity. Figure 3.5 shows the effect of the pixel sensitivity correction on an image. Figure 3.6 shows the effect of the pixel sensitivity correction on the actual pixel intensity values on row 50 of the images shown in figure 3.5.

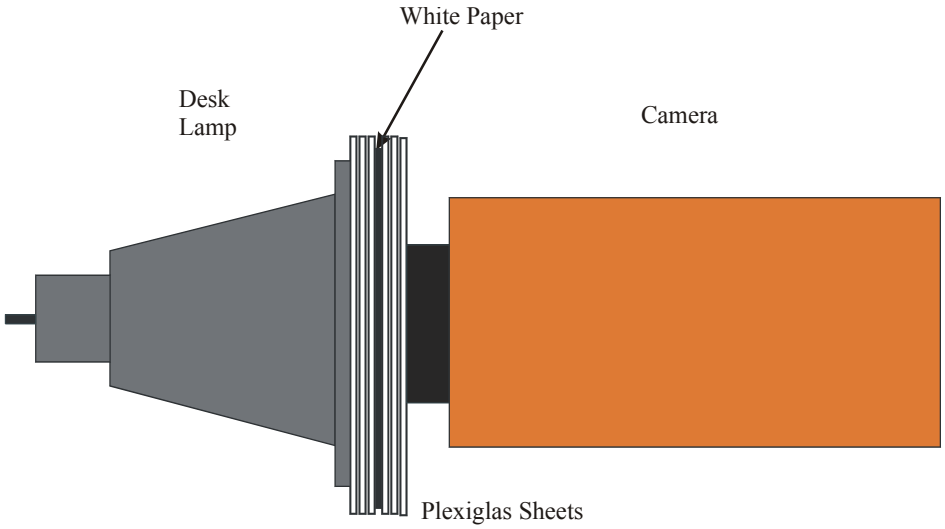

Figure 3.4: Setup used to acquire pixel sensitivity correction images.

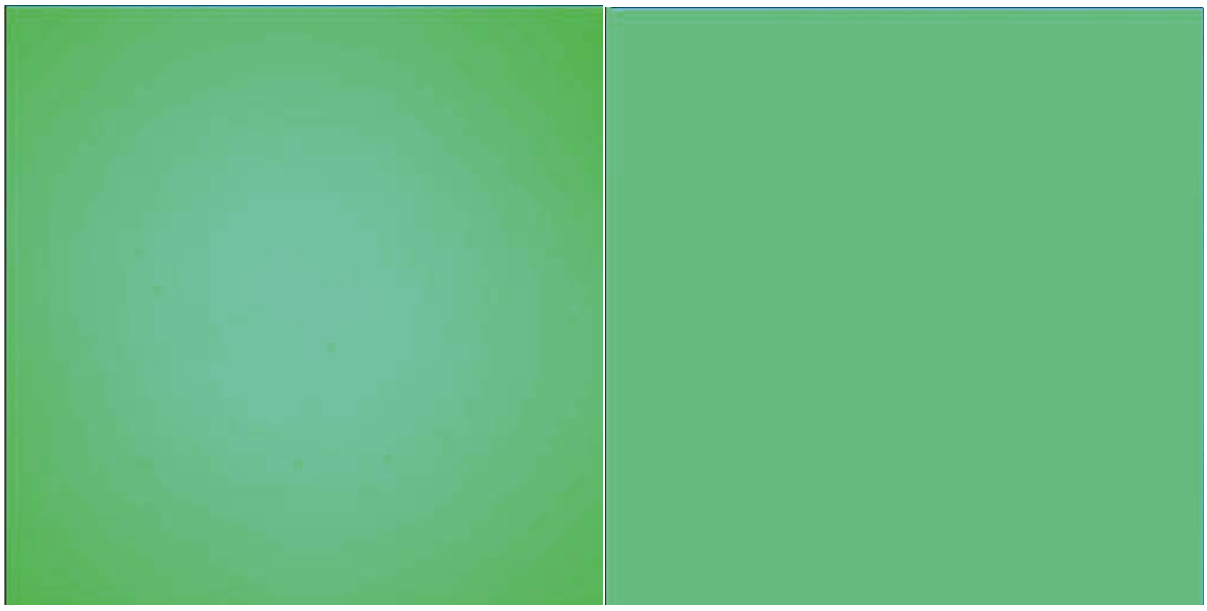

(a) (b)

Figure 3.5: Demonstration of pixel sensitivity correction. Figure (a) shows a colorized pixel sensitivity image before correction and figure (b) shows the same image after correction.

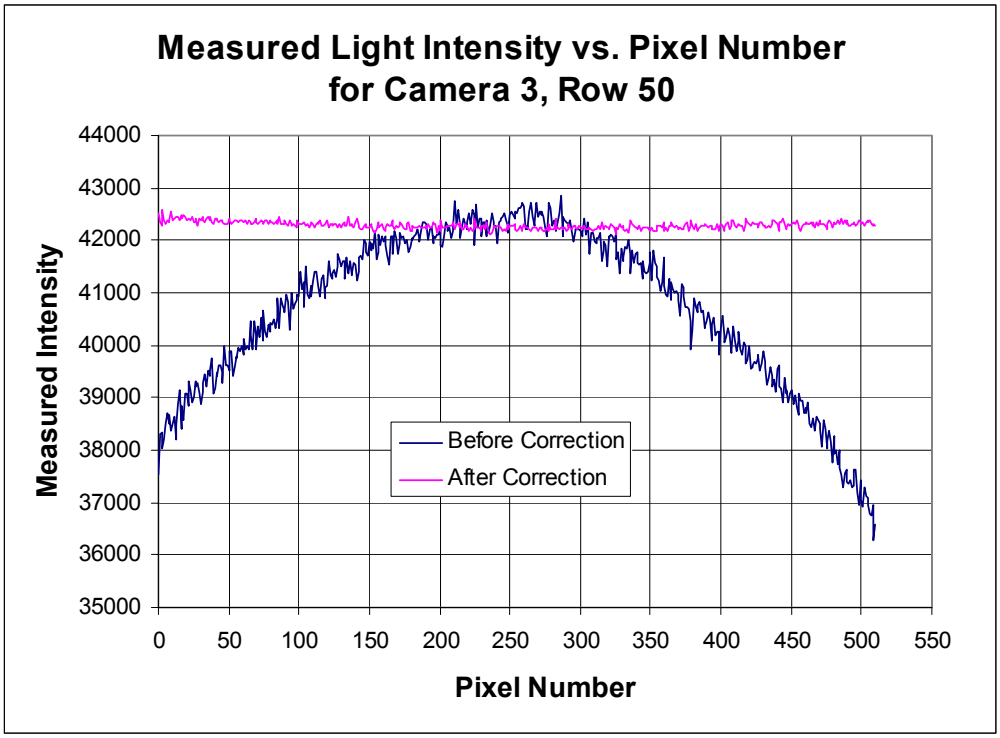

Figure 3.6: Measured light intensity versus pixel number, for row 50 of camera 3, before and after pixel sensitivity correction.

3.4.4 White Card Correction

The image passing through the iodine cell passes through two windows as well as the iodine gas inside the cell. These windows reflect and absorb a portion of the light passing through the iodine cell. The reference image does not pass through any windows and thus it does not loose the same portion of light. The end result of the loss of this reflected and absorbed light is that the ratio of the filtered and reference pixel intensities will be lower than what would be the case if the filtered image did not pass through the windows on the ends of the iodine cell. In addition to the losses due to the filtered images passing through these windows there potentially are global variations in sensitivity to light from camera to camera, so a method must be developed to correct for this as well. The procedure used to correct for these potential sources of error is called white card correction for reasons that will be explained below.

The correction used to account for the differences in light intensity recorded by each camera module due to the windows on the iodine cell and differences in the overall light sensitivity of each camera is called a white card correction because a set of images of a solid white card are acquired as part of the procedure used to perform this correction. The card is illuminated by the laser, which is fired at a constant optical frequency while the white card correction images are acquired. An iodine

cell calibration must be performed before the white card correction images are acquired, because the white card correction images must be acquired at an optical frequency where the mean transmission ratio between the filtered and reference views is at a global maximum. The physical setup used to acquire iodine cell calibration images is the same as the setup used to acquire white card correction images. Once the white card correction images are acquired and averaged to generate an average white card correction image, all of the other image corrections described above are performed. First, the average background image is subtracted from the average white card image. Next, the pixel sensitivity correction is applied to the entire image. After this step, the filtered image is vertically mirrored because prior to this the filtered image appears to be a mirror image of the reference image. Next, each warped region of interest is mapped to its corresponding rectangular region of interest. Once the two regions of interest have been de-warped, a pixel filter is applied to each region of interest. Finally, an array of white card ratios is calculated for each camera module, from the pixels in the filtered and reference regions of interest. Ideally, these ratios should all be unity, but for the reasons described in the first paragraph of this section this ratio is less than unity. The procedure used to calculate this array of white card ratios for each camera module also calculates an average white card ratio for each camera module. While the array of white card ratios and the average white card ratio for each camera module are saved in a data file the average white card ratio for the camera module to be used to monitor the laser frequency variations should be recorded by the user for later use. The white card correction is applied to an image by dividing each pixel in the image by the corresponding white card correction ratio. Figure 3.7 shows the results of an iodine cell calibration before the white card correction is applied and figure 3.8 shows the results of the same iodine cell calibration after the white card correction has been applied.

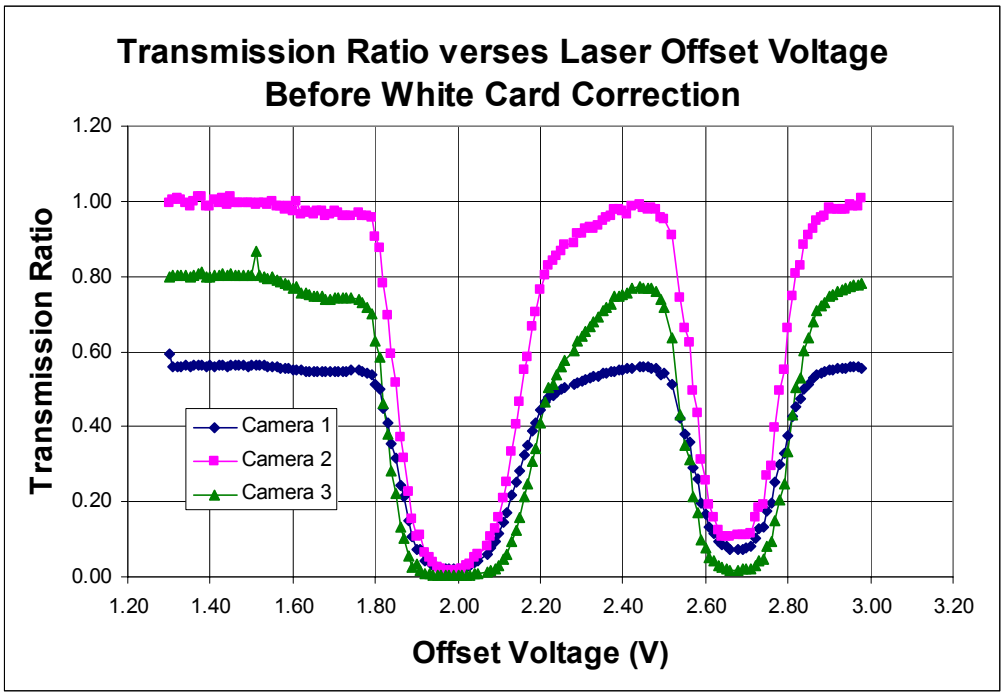

Figure 3.7: Results from iodine cell calibration before white card correction.

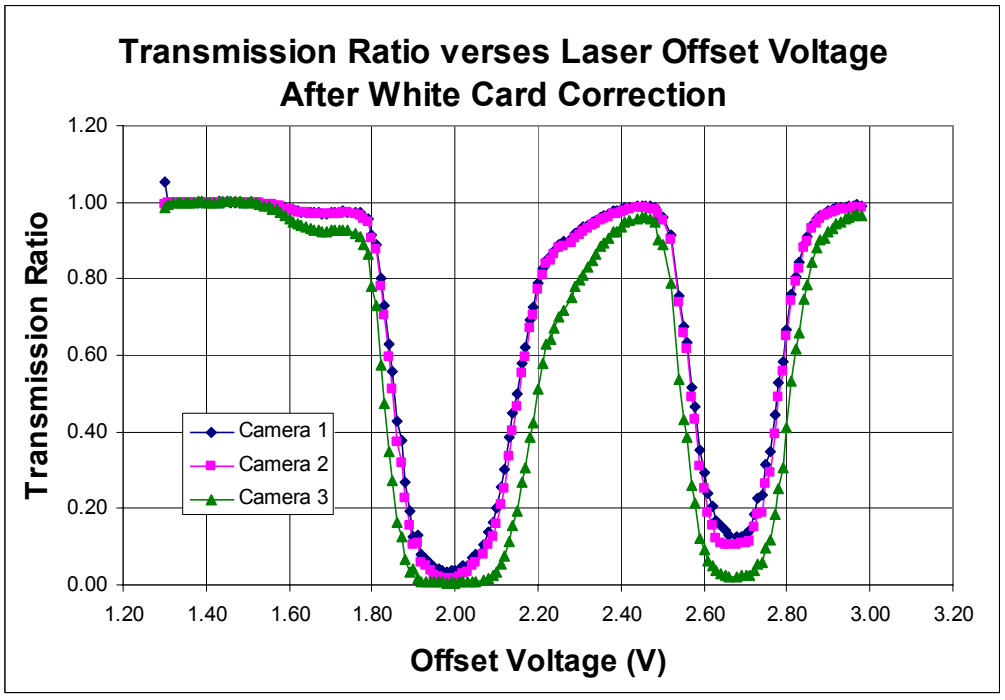

Figure 3.8: Results from iodine cell calibration after white card correction.

3.5 Camera Module Viewing Angles

The MATLAB toolbox, *"Camera Calibration Toolbox for MATLAB"*, written by Jean-Yves Bouguet, was used in previous tests of the VT DGV system to determine the camera module viewing angles needed to reduce acquired velocity data.[83] In these previous tests it was necessary to manually enter the dot center locations from the dot grid images into a data file. This data file was used by the MATLAB Toolbox to determine camera calibration parameters in addition to determining the rotation matrix needed to calculate the camera module viewing angles. To achieve the best results, a series of at least 10 different images at 10 different viewing angles should be used. Manually entering 10 sets of dot center locations took roughly 32 hours, which proved to be an unacceptable length of time for this task. A single error in data entry could prevent the toolbox from determining the viewing angles, thus making it necessary to spend precious time looking for errors. The MATLAB Camera Calibration toolbox had an automatic corner extraction program, which would automatically determine the corner locations for a series of images of a checkerboard grid. Since manually entering dot center locations was both very time consuming and error prone, the target used while acquiring dot grid images was changed from a pattern of dots to a checkerboard grid. This reduced the amount of time needed to determine the viewing angles from days to mere minutes!!

The first step in determining the viewing angles was to acquire 10 images of a checkerboard pattern from ten different viewing perspectives for each camera module. The images acquired by the DGV system cannot be directly plugged into the camera calibration toolbox so these images were exported from the DGV control program file format into the Flexible Image Transport System (FITS) file format. The FITS format images were then opened in an image viewing program provided by the manufacturer of cameras 1 and 3, Spectra Source. Once open the images were vertically mirrored and then saved in the Tag Image File (TIF) file format. The TIF images could then be used in the camera calibration toolbox. The first step in this procedure was to extract the corner locations on each of the ten images for a given camera module. This was done automatically for the most part. The user only needed to select the four outer corners of the area to be used in the camera calibration. It was important to consistently select these points in the same order and note the order in which the points were selected because the order in which the points were selected also determined the orientation of the coordinate system attached to the checkerboard pattern and hence the data plane. During this research, the points were selected in the following order: upper left corner, upper right corner, lower right corner, and finally lower left corner. This oriented the coordinate reference frame attached to the data plane in the following manner. The origin was located at the upper left corner. The positive x axis pointed down toward the lower left corner of the data plane. The positive y axis

pointed to the right toward the upper right hand corner of the data plane. Finally, the positive z axis pointed out of the data plane according to the right hand rule. The portion of the camera calibration toolbox which calculated distortion and principal point for the camera was disabled because these parameters could not be calculated because of the large distance between the camera modules and the data plane. These parameters were disabled by setting the parameters: center_optim = 0 and est_dist = (0; 0; 0; 0; 0) in the camera calibration toolbox. Once the corners were extracted for the set of images from a given camera module, and the routines to calculate distortion and principal point were disabled, the camera calibration was performed. This calibration was still able to determine quantities such as the focal point and pixel error.

Once the calibration was performed, the geometric correction image from which the viewing angles were to be determined was opened and the corners for that image were extracted using the same procedure described above. Next, the extrinsic properties of this image were calculated. These properties included a translation vector, a rotation vector, and a rotation matrix to transform the coordinate system from the reference frame attached to the data plane to the reference frame attached to the camera module. The rotation matrix was used to determine the Euler angles associated with the coordinate transformation between the camera module reference frame and the data plane reference frame. The origin for the camera module reference frame was located at pixel 0,0 in the upper left corner of the image. The positive x axis for the camera module reference frame pointed toward the upper right corner of the image along the top row of image pixels. The positive y axis for the camera module reference frame pointed toward the lower left hand corner of the image along the first column of image pixels on the left side of the image. The positive z axis pointed in the direction the camera was viewing according to the right hand rule. The rotation matrix had the following form:

$$R = \begin{bmatrix} r_{11} & r_{12} & r_{13} \\ r_{21} & r_{22} & r_{23} \\ r_{31} & r_{32} & r_{33} \end{bmatrix} \tag{5}$$

Assuming the rotation was a 3, 2, 1 (z, y, x) rotation, values in this matrix would have the following form:

$$R = \begin{bmatrix} \cos\theta_y \cos\theta_z & \cos\theta_y \sin\theta_z & -\sin\theta_y \\ (\sin\theta_x \sin\theta_y \cos\theta_z - \cos\theta_x \sin\theta_z) & (\sin\theta_x \sin\theta_y \sin\theta_z - \cos\theta_x \cos\theta_z) & \sin\theta_x \cos\theta_y \\ (\cos\theta_x \sin\theta_y \cos\theta_z - \sin\theta_x \sin\theta_z) & (\cos\theta_x \sin\theta_y \sin\theta_z - \sin\theta_x \cos\theta_z) & \cos\theta_x \cos\theta_y \end{bmatrix} \tag{6}$$

Therefore, the value in $r_{11} = \cos\theta_y \cos\theta_z$, the value in $r_{12} = \cos\theta_y \sin\theta_z$ and so on. The value of the Euler angle θ_y was determined using r_{13} as follows:

$$\theta_{y1} = -\sin^{-1}(r_{13}) \tag{7}$$

or

$$\theta_{y2} = \pi - \sin^{-1}(r_{13}) \tag{8}$$

Equation 7 was derived from the fact that arcsine is periodic with a range of $\pi/2$. These two angles were used to determine four possible values for θ_z using r_{12}:

$$\theta_z = \begin{bmatrix} \dfrac{\sin^{-1}(r_{12})}{\cos\theta_{y1}} & \pi - \dfrac{\sin^{-1}(r_{12})}{\cos\theta_{y1}} \\ \dfrac{\sin^{-1}(r_{12})}{\cos\theta_{y2}} & \pi - \dfrac{\sin^{-1}(r_{12})}{\cos\theta_{y2}} \end{bmatrix} \tag{9}$$

The same procedure was used to determine four possible values for θ_x using r_{23}:

$$\theta_x = \begin{bmatrix} \dfrac{\sin^{-1}(r_{23})}{\cos\theta_{y1}} & \pi - \dfrac{\sin^{-1}(r_{23})}{\cos\theta_{y1}} \\ \dfrac{\sin^{-1}(r_{23})}{\cos\theta_{y2}} & \pi - \dfrac{\sin^{-1}(r_{23})}{\cos\theta_{y2}} + \pi \end{bmatrix} \tag{10}$$

The four sets of angles were compared to the remaining values in the matrix R to determine which sets were possible Euler angles for the rotation matrix R. Generally two of the sets of angles did not match the other values in R and the two remaining sets matched the other values in R. The two sets that matched had the same angular displacement but the rotation was in opposite directions so either set of angles would have worked in the DGV data reduction program. The set of smaller Euler angle values was generally chosen to be used in the data reduction program.

An additional step was needed to correct for a difference in the orientation of the reference frame attached to the data plane by the calibration toolbox and the orientation of this frame desired for the DGV data reduction program. The following rotations were added to the Euler angles to account for this difference:

$$\theta_x = \theta_x' - \pi \tag{11}$$

$$\theta_y = -\theta_y' \tag{12}$$

$$\theta_z = \theta_z' - \frac{\pi}{2} \tag{13}$$

where θ_x, θ_y, and θ_z are the corrected Euler angles, and θ_x', θ_y', and θ_z' are the Euler angles directly from the rotation matrix output by the calibration toolbox. Another adjustment was also

needed because the rotation matrix output by the camera calibration toolbox was for a coordinate transformation from the data plane reference frame to the camera reference frame. The desired coordinate transformation is from the camera reference frame to the data plane reference frame. The direction of the transformation can be changed by multiplying each of the Euler angles calculated above by -1. This puts the Euler angles into the final form needed to input them into the VT DGV data reduction procedure.

3.6 Iodine Cell Calibration

The manufacturer of the Nd:YAG laser used in this research provided an easy way to change the optical frequency for the laser. A DC offset voltage could be sent to the laser to vary the optical frequency. Unfortunately the range of frequencies and the actual optical frequency associated with a given offset voltage varied depending on the operating conditions, such as ambient temperature, in the area where the laser was being fired and the settings for various adjustments on the seed laser inside the Nd:YAG host laser. The successful use of the DGV technique depended on a specific transmission ratio calculated from the reference and filtered views of a given camera module being associated with a specific optical frequency. Therefore, each of the camera modules was calibrated to determine the relationships between the transmission ratio, offset voltage, and the optical frequency of the light captured by the camera module. The procedure used to acquire these "iodine cell calibrations", as they are often called, will be described in the rest of this section.

The first two steps in acquiring iodine cell calibration data were to acquire geometric and background images for each of the camera modules being calibrated. The checkerboard pattern used to acquire the geometric correction images was illuminated by a desk lamp. For the background images, the laser was turned on and enabled so a beam was produced, but the beam was diverted to a beam dump instead of being directed into the data area. Every effort was made to eliminate any other possible light sources while these images were being acquired and while the iodine cell calibration was being performed. This was done to maximize the dynamic range of the camera modules. The pixel sensitivity of each camera did not need to be measured prior to each iodine cell calibration or DGV data acquisition so this procedure assumes that the pixel sensitivity was determined prior to performing each iodine cell calibration. Another objective of the iodine cell calibration was to determine the offset voltage where the transmission ratio calculated from the reference and filtered views of each camera was at a maximum value so this offset voltage could be used when the white card correction images were acquired. Once the geometric and background correction images were acquired and averaged, the average geometric correction images were used to determine the warp

points and rectangular regions of interest for each camera module. The data area selected by the warp points was the same for all of the camera modules used in the calibration. This data area was the same size and covered the same area where DGV data was to be collected. All of the rectangular regions of interest for the camera modules used to acquire the iodine cell calibration were also the same size. This was done so the data area associated with the size of a pixel would be the same for all of the camera modules. During this research these rectangular regions of interest were each 350 pixels wide and 250 pixels high. The size of the data area used in this research was 0.1778 m x 0.127 m (7 inches x 5 inches).

Once the geometric and background correction images were acquired and the warp points and rectangular regions of interest were selected the system was prepared to acquire an iodine cell calibration. The offset voltage was set to the starting voltage for the calibration. The laser needed to be run at this offset voltage for about 5 minutes so the laser could settle on the commanded optical frequency. This length of time was only needed when the offset voltage was set to the starting voltage, because this usually was a large change in the optical frequency. The laser could lock on to a commanded optical frequency faster if the commanded optical frequency was close to the optical frequency the laser was previously operating at. Next, the laser beam was steered through a set of optics to form a cone of laser light which was used to illuminate the target. The target was the front surface of the calibration wheel if wheel data was to be acquired. The target was a flat plate covered with 600 grit sandpaper and painted white for the cases where flow data was to be acquired. Next, the range of offset voltages to be scanned during the calibration and the number of increments desired for the calibration were set in the DGV control program. Once these values had been set the calibration was started.

The DGV control program used the voltage range and number of increments to determine the needed change in offset voltage between the increments. An image was acquired by each of the camera modules being calibrated at each voltage increment. The user could select the length of time the program paused between acquiring images. This was important because the laser required a few seconds to lock on to the new commanded optical frequency after the offset voltage was changed. Usually, the control program was set up to wait approximately 12 to 15 seconds after the offset voltage was changed before acquiring the calibration image. The actual number of images acquired was n+1 where n was the number of increments since the first image from each camera module was acquired at the starting offset voltage. The number of images acquired for an iodine cell calibration depended on the size of the voltage range over which the calibration was being conducted and the

desired resolution. A general rule of thumb was to use 50 images for every 0.5 volts. This could be, and was, stretched to as few as 25 images for every 0.5 volts but this sacrificed calibration resolution. Figure 3.9 is a drawing which shows the setup of the DGV system in the Virginia Tech Stability Wind Tunnel during an iodine cell calibration and during calibration wheel velocity data acquisition. The procedure used to reduce the iodine cell calibration images will be discussed in Chapter 4.

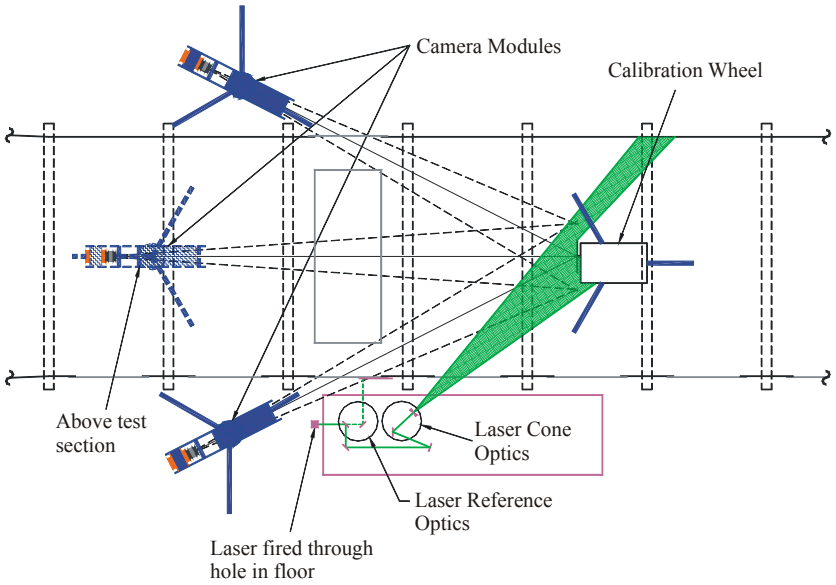

Figure 3.9: DGV system setup in the Virginia Tech Stability Wind Tunnel. This setup was used to acquire iodine cell calibrations and calibration wheel velocity data.

The main drawback to this technique for calibrating the camera modules was that the calibrations were quite time consuming. The normal size of a calibration scan was between 150 and 200 increments. A 151 point scan (150 increments) required roughly 1 hour and 15 minutes to acquire all of the calibration images. The degree to which the calibration was successful was not known until all of the calibration images had been acquired and reduced. Also, a single calibration did not provide enough information to determine all of the information needed to use the DGV system to acquire velocity data. Usually large, coarse scans were used to determine the location of interesting absorption features. Next, large scans over a more narrow offset voltage range were used to identify specific absorption characteristics. These scans used the rule of thumb described above to determine the number of increments to be used. Finally, a scan of roughly 100 images over a small voltage range (roughly 0.5 volts usually) was used to calculate the relationship between transmission ratio from each camera module and optical frequency. The problem with the length of time required to perform an iodine cell calibration was compounded by other problems with the Nd:YAG laser performance and with two of the 16-bit digital cameras used in the VT DGV system. The problems

with the laser and the digital cameras will be discussed in greater detail in Chapter 5. The end result of the laser and camera problems in addition to the length of time required to perform an iodine cell calibration was that an attempt to acquire DGV velocity data required 10 to 12 hours of work if everything worked as expected.

3.7 Calibration Wheel Data Acquisition

Once the iodine cell calibration was acquired and reduced and the white card correction ratio was determined for each camera module, the laser offset voltage was set so the transmission ratio for the camera modules was roughly 0.5 on the iodine absorption feature chosen for use in acquiring DGV velocity data. This maximized the sensitivity of each camera module to changes in optical frequency due to laser light being reflected off of a moving particle or surface. Next, the beam dump was moved into place to keep the laser beam from entering the data area. This was done so geometric and background correction images could be acquired while the laser continued to run. After these correction images were acquired the beam dump was removed and a series of 10 images were acquired by each camera module with the wheel stationary. These images were averaged to generate an average stationary wheel image for each camera module. These average images were used to determine a reference value for the transmission ratio of each camera module at the current offset voltage, as part of the DGV data reduction procedure. Next the calibration wheel was started and was allowed to run approximately 1 minute before DGV data acquisition began. A set of 50 DGV velocity images were acquired during each attempt to acquire calibration wheel data. The DGV control program waited approximately 10 seconds between each acquired image. The output voltage from the calibration wheel motor controller was acquired and averaged while each image was acquired. This voltage was used to independently measure the calibration wheel angular velocity. Three attempts were made to acquire calibration wheel data. The data from the first two attempts were judged to be unreliable because of problems with the performance of the Nd:YAG laser. The third set of calibration wheel data had the best chance of being usable so this set was closely scrutinized and reduced. The procedure used to reduce the calibration wheel data will be discussed in Chapter 4.

3.8 6:1 Prolate Spheroid Data Acquisition

Once a reliable set of calibration wheel data was acquired, an attempt was made to acquire DGV velocity data in the wake of a 6:1 prolate spheroid. This attempt required the positions and viewing angles of the camera modules to be adjusted slightly. It also required some additional laser optics to be set up to form a thin sheet of laser light perpendicular to the major axis of the prolate

spheroid at approximately 77% (1.059 m) down the length of the prolate spheroid. Figure 3.10 shows the laser optics setup used to form the laser sheet. A series of geometric and background correction images were acquired for the new camera module positions and a series of iodine cell calibrations were performed to determine the location of the iodine absorption feature to be used to acquire DGV velocity data. A special tripod was used to hold the checkerboard pattern and the solid white target plate in place where the data plane was located above the prolate spheroid. The white target was used

Figure 3.10: Setup for the laser optics used to form the laser sheet.

while iodine cell calibrations and white card correction images were acquired. The same optics used previously to illuminate the data plane with a cone of laser light were used while these images were acquired. Due to problems with the Nd:YAG laser, several attempts were required to acquire a usable iodine cell calibration. As was the case with the procedure used to acquire calibration wheel data, after the iodine cell calibration images and white card correction images had been successfully acquired and reduced, the laser was set to the offset voltage needed to make the mean transmission ratio, calculated from the filtered and reference views of the three camera modules, roughly 0.5. Once the laser offset voltage was set so the mean transmission ratio for each of the camera modules was roughly 0.5, a series of 10 images of the white target plate illuminated by the Nd:YAG laser was acquired. Next, the beam dump was moved into place to keep the laser beam from entering the data area and geometric correction images were acquired while the laser continued to run. Next, the tripod used to hold the checkerboard pattern and white target plate was removed from the wind tunnel test section. Once the tripod was removed, the beam stop was removed from the laser path and the laser

beam was diverted from the cone optics to the optics used to form the laser sheet in the data plane. Once the laser sheet was formed above the prolate spheroid model, the background correction images were acquired with the wind tunnel fan off and the smoke machine off. The background correction images were acquired in this way to correct for laser light reflecting off of the model and the far wall of the wind tunnel test section.[84] Next, the wind tunnel fan was started and the speed of the fan was increased until the dynamic pressure in the wind tunnel test section was 10.16 centimeters of water (4 inches of water). Once the desired dynamic pressure was reached, the smoke machine used to inject seed particles into the flow was enabled. Once the smoke machine began to inject smoke into the wind tunnel, a series of test images were acquired to see if the camera modules were capturing enough light scattered by the smoke to acquire instantaneous DGV velocity data. Unfortunately this was not the case. Images were acquired at several different fan speeds down to a dynamic pressure of 2.3 inches of water. None of the acquired images gathered enough reflected light to measure a frequency shift. The attempt to acquire DGV flow velocity data was stopped when the smoke in the wind tunnel became too thick to continue. Unfortunately, due to problems with the Nd:YAG laser and 16-bit cameras another attempt could not be made. The problems encountered with the Nd:YAG laser and the digital cameras will be discussed in greater detail in Chapter 5. Figure 3.11 is a drawing showing the setup of the VT DGV system used in the attempt to acquire DGV velocity data in the wake of a 6:1 prolate spheroid.

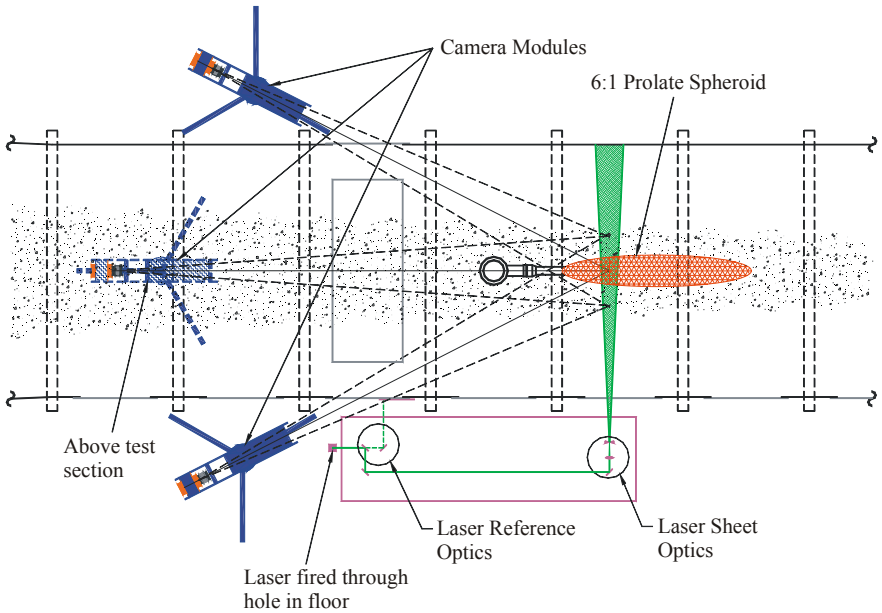

Figure 3.11: VT DGV system setup used to attempt to acquire DGV velocity data in the wake of a 6:1 prolate spheroid.

Chapter 4: Data Reduction